Electroless Plating of Thin Silver Films on Porous Al$_2$O$_3$ Substrate and the Study of Deposition Kinetics

Fang Mei, Donglu Shi[**]

Department of Chemical and Materials Engineering, University of Cincinnati, Cincinnati, OH 45221-0012, USA

Abstract: A novel concept has been developed to coat the inner pore surfaces of reticulated alumina with a thin silver film by an electroless-plating method. As a result of coating, the porous alumina sample exhibits a sharp transition from insulating to conducting due to a thin silver layer on the inner pore surfaces. Systematic studies have been carried out to investigate the coating kinetics by employment of scanning electron microscope (SEM), X-ray diffraction (XRD), and computer simulation. Both coating procedures and effects of processing parameters on the quality of films are reported. Also, this paper presents the film bonding strength to the substrate, effects of sintering, and conduction mechanism of coated composite. The fundamental silver electroless-plating mechanism has been identified based on computer modeling. The simulation results indicate an excellent agreement between the silver deposition behavior and the physical model applied.

Key words: electroless plating; thin silver films; deposition kinetics

Introduction

There have been extensive reports on the coating of metallic films on ceramic substrates. In previous studies, the research mainly focused on coating of the two-dimensional surface of a substrate. Jayaraman[1] deposited an ultra-thin metallic membrane on ceramic supports for hydrogen separation by sputtering method. Padilla et al.[2] synthesized a silver membrane on outer surface of the porous ceramic with average pore size of 4 μm, which was much smaller than that in this study, and applied it for water treatment. Jiang et al.[3,4] had pioneered a novel method for coating a hydroxyapatitie film onto porous alumina for hard tissue prosthetics. However, coating of a conducting film onto the inner pore surfaces of reticulated ceramics for high conductivity has never been reported before.

Reticulated ceramics, especially porous alumina, had been widely used as an effective filter material in water treatment and other areas[5,6]. The most common applications of porous ceramics, also called reticulated ceramics, are molten-metal and diesel engine exhaust filters. It can also be used as catalyst supports and industrial hot-gas filters, thermal insulators, and gas combustion burners. Structurally, a reticulated material is a porous matrix comprised of interconnected voids surrounded by a web of ceramic, metal, or polymer. These porous network structures have relatively low mass, low density, and low thermal conductivity. The open-cell nature of reticulated materials is a unique characteristic essential in many applications. However, the surface-to-volume ratio of reticulated materials is much larger than that of the dense materials, making them ideal for surface reaction applications.

The unique feature in this study is the conductive

coating on the inner pore surfaces of the ceramic substrate. Several functions can be served by this conductive coating: 1) the coating, although quite thin (several microns), can induce high conductivity of the entire ceramic substrate leading to an insulating-to-conducting behavior; 2) an electrical field can be applied to the silver coating, creating a physical driving force required in the filtration process; and 3) such a porous material, compared to the dense materials, has the following advantages: large surface area, high flux rate, superb mechanical strength, and excellent chemical stability. For instance, one of the applications is the entrapment of ionic particles in water treatment[7]. In this study, we report coating the silver film onto the inner pore surfaces of reticulated alumina by using an electroless-plating method. We present experimental data on coating process, microstructure of the film, and the electrical properties of the coated composite. Also, we present the computer modeling of the silver deposition process.

1 Experimental

There are many well-developed coating methods such as sputtering, sol-gel, spin coating, dip coating, and chemical vapor deposition (CVD), but few can be used for coating the inner pore surfaces of the porous materials. To coat a film on the inner pore surfaces inside the substrate, the coating materials must penetrate the entire substrate and deposit the precursors on the inner pore surfaces uniformly. In addition to other types of liquid coating techniques, electroless coating can be an effective approach for coating the porous alumina. The goal of this study was to deposit a conductive layer (silver) onto the inner surfaces of the pores in a strong and chemically stable substrate. The substrate materials identified in this study were commercially reticulated alumina manufactured by ALUCEL™, High Tech. Ceramics, Alfred, NY. The substrate was of 94% alumina and was made by a sponge method[8]. Pore size was 10 PPI (pores per inch), and porosity was 80%. Dense alumina plates were also used in parallel treatment for comparison purposes. These were commercial plates from Coors Ceramicon Designs. In this study, the samples were cut into 1 cm×1 cm×0.2 cm for dense alumina and 1 cm×1 cm×1 cm for porous alumina.

The bond strength of the film to the substrate was

very sensitive to the contaminant on the surface, so the substrate was rinsed thoroughly with alcohol first, and then immersed in CrO_3 solution and ultrasonically degreased before it was coated. The substrate was then cleaned by deionized (DI) water and dried in oven.

Electroless plating using Co (II) as a reducing agent was a novel method developed in recent year[9]. The solution was prepared in the following steps: 2 parts 3.5 mol/L $(NH_4)_2SO_4$ solution and 1 part 25% $NH_3 \cdot H_2O$ were added into 2 parts 0.14 mol/L $AgNO_3$ solution, and then 2 parts 0.35 mol/L $CoSO_4$ was added. DI water must be used to prepare the solution; otherwise, the ions in the water would combine the Ag^+ and produce insoluble precipitation. To accelerate the coating process, 0.15 g/L KBr was used as an accelerator.

After the substrate was rinsed, degreased, and dried, it was sensitized in Sn (II) solution (2 g/L) for 10 min, rinsed with DI water, and then was activated in 10 g/L $AgNO_3$ for 10 min. The additional $AgNO_3$ solution inside the pores was removed before it was immersed in the main plating solution. The plating process was carried out at room temperature, and the plating load and the plating time depended on the film thickness needed.

The morphology and the thickness of the silver film were investigated by using a Joel scanning electron microscope (SEM). The grain growth rate of silver was calculated by measuring the grain size from the SEM photographs. A Philip X-ray diffractometer with Cu Kα radiation was used to carry out the structural investigation. Electrical resistivity was measured by a QuadTech MegOhmmeter Tester. The conductive silver paint was used to attach the current leads, which was carried out by painting two parallel surfaces of the porous sample uniformly with silver paint ensuring an even current density across the cubic sample.

2 Results and Discussion

2.1 Electroless plating

It was found that KBr could not only accelerate the reduction of Ag^+, but also make the film more uniform and dense. For the solution without KBr, it was difficult to obtain a uniform and continuous silver film. Figure 1 shows the silver coatings on dense alumina with (Figs. 1a and 1c) and without (Figs. 1b and 1d) KBr accelerator. The plating time of 10 min was kept

the same for both samples. Note that the large visible grains from Figs. 1b and 1d (Figs. 1b and 1d are the same sample area but with different magnifications) are in fact grains of alumina. The silver grains appear in extremely small white dots dispersed on large alumina grains. These microstructures suggested that it
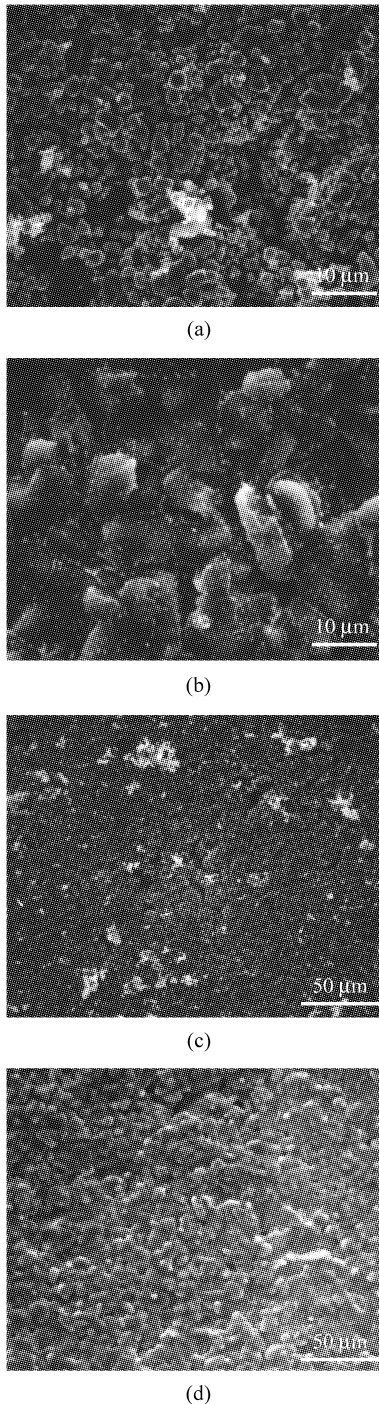

(a)

(b)

(c)

(d)

Fig. 1 Influence of accelerator (KBr) on plating results. (a) and (c), plating with KBr accelerator, and (b) and (d), without using KBr accelerator

was necessary to use KBr as an accelerator in the plating process.

In contrast, Figs. 1a and 1c (again these are from the same sample area but with different magnifications) show a uniform silver film with grain sizes of 3-4 μm on the alumina substrate, while without KBr, the silver grains could hardly be seen from the alumina substrate. Therefore, accelerator was used for all other plating processes in this study.

Silver was also deposited on porous alumina substrate using the plating solution by reducing Ag^+. This ensured that all the surfaces in contact with the solution could be coated evenly. Figure 2 shows the SEM photographs of the cross sections of the porous substrate after plating. It can be seen that there is no considerable deviation of film thickness in different directions. As indicated in these SEM images, the alumina substrate appears to be white while the silver coating exhibits darker gray contrast. From these images it can also be seen that the silver film is quite uniform through out the entire cross sectional area of the pores.
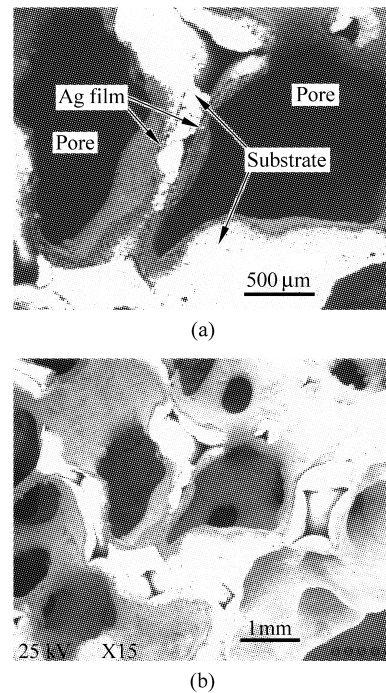

(a)

(b)

Fig. 2 SEM photographs showing the cross sections of coated silver films on the inner surfaces of the pores

2.2 Silver film deposition kinetics

It was easier to study the silver coating morphology on

the dense substrate. It is noted here that for both dense and porous substrates, the plating conditions were kept exactly the same. Therefore, useful information can be learned from examining the coatings on the dense substrate. Figure 3 shows the SEM photographs of film coated on a dense substrate. The main part of the silver film was a uniform crystalline layer with grain size about 3 μm, except for some minor pores. The silver grains were of nearly spherical shape, which indicates the similar growth rate in all directions.
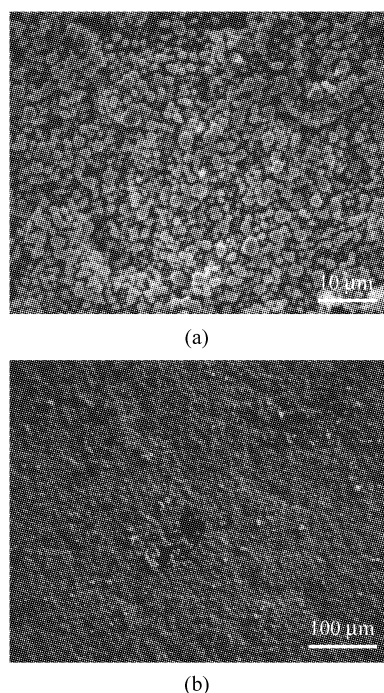

(a)

(b)

Fig. 3 SEM photographs showing the morphology of silver film on dense substrates

The grain growth morphology is shown in Fig. 4. These are SEM images of the silver coating on dense substrate for different plating times. Note that, in Figs. 4a and 4a′, the large grains are the dense alumina substrate. The silver grains appear in these photographs as very small white dots dispersed in the large alumina grains. As the plating time prolongs, the silver grains grow larger and even cluster locally as can be clearly seen in Figs. 4d and 4d′. By measuring the average grain size with different plating time, we can plot the curve of grain size versus plating time (Fig. 5). At the beginning of the plating process, some silver particles were formed randomly on the substrate and grew almost linearly with time (Figs. 4a and 4a′). Then more small silver particles appeared and these separated grains grew larger as plating time increased (Figs.

4b and 4b′). Finally, these grains came in contact each other and a continuous film was formed (Figs. 4c and 4c′). After the first layer of silver film was formed, some grains grew above it and formed silver particle clusters (Figs. 4d and 4d′). During the prolonged plating, silver ions in the solution became diluted and eventually reached a low level at which the grain growth saturated as can be seen in Fig. 5.

2.3 Resistivity measurements

In Fig. 6 the overall resistivity of the porous composite is plotted against the plating time. As can be seen in Fig. 6, there is a clear transition from insulating to metallic conducting behavior beginning at plating time of 8 min and finishing at 12 min. This indicates that the silver grains have come to a full contact at 12 min, which, as can be seen in Fig. 5, is about the grain growth saturation time. There appears to be four stages in the resistivity versus plating time plot in Fig. 6. 1) At the beginning, the substrate is insulating before any deposition of the silver film. Up to about 6 min, although SEM has revealed silver particles on the alumina substrate, the resistivity remains a constant; 2) the resistivity begins to decrease more noticeably after 6 min; 3) at 8 min, resistivity decreases dramatically, indicating that a large fraction of silver grain impingement has occurred; and 4) the resistivity continues to decrease after 10 min but in a more gradual fashion.

In stage 1, some silver particles began to deposit on the substrate, but they were separated from each other (Fig. 4a). In this way, the electrical current was not able to pass through the separated grains until a path was formed, so the silver grains did not contribute to conductivity at this stage. The resistance of the substrate was in fact of the same value as before the substrate was coated. In stage 2, as the plating continued, more grains were formed and the grain size increased. Some grew large to connect with each other in localized areas (Fig. 4b). At certain point, a percolation path was formed, and the silver film began to transport electrical current. However, the overall cross sectional area of the silver path was still small which only slightly suppressed resistivity. In the third stage, as soon as substantial silver grains came in contact, the resistivity experienced a sharp drop at 8 min (Fig. 4c). After a continuous first layer film was formed, the plating
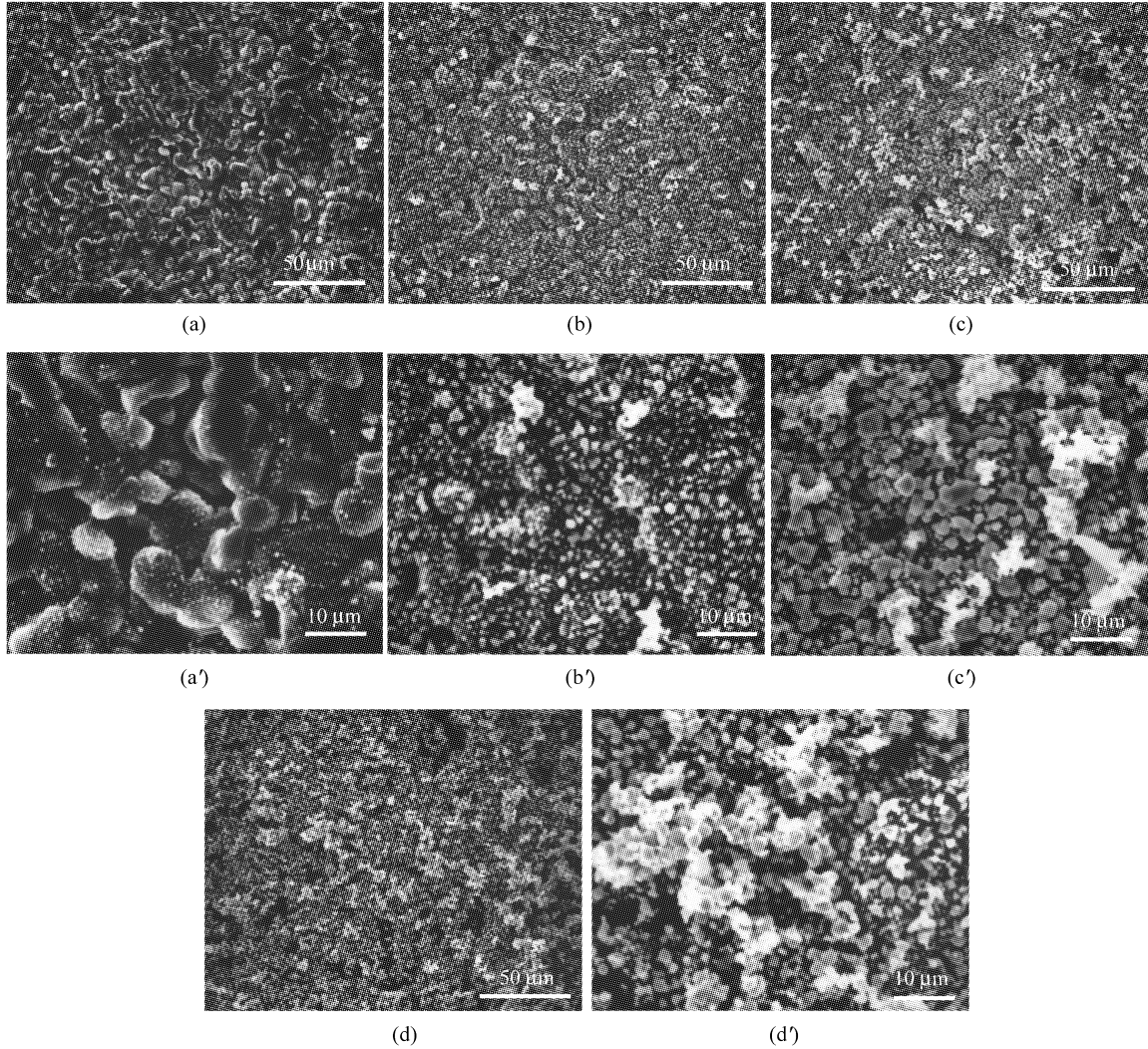
Fig. 4   SEM photographs showing the growth of silver grains plating with time. (a) 2 min; (b) 6 min; (c) 12 min; and (d) 24 min. Note that (a′), (b′), (c′), and (d′) are the corresponding images with high magnifications.
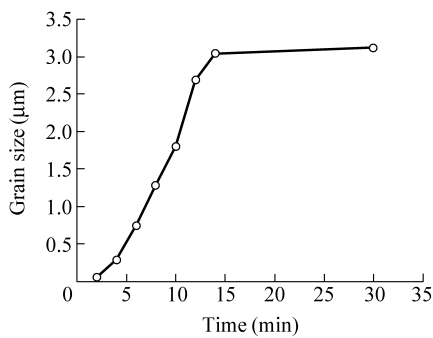

Fig. 5   Silver grain size versus plating time for the samples shown in Fig. 4

process came into the last stage. At this stage, the resistivity was merely affected by the increase in the silver film thickness. However, the thickness change

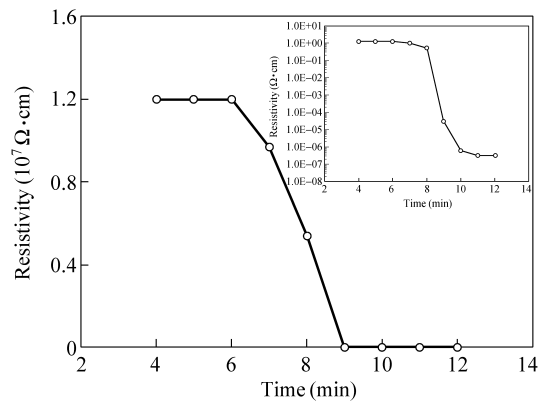had much smaller effect on resistivity as   shown   in Fig. 6. Finally, the resistivity saturated due to the

Fig. 6   Resistivity versus plating time for silver coated porous alumina

depletion of the plating solution. No more silver could be deposited from the solution. Therefore, to further increase the film thickness, a new solution was needed.

2.4 XRD characterization

As a result of surface roughness of the porous alumina, the signal of X-ray diffraction of the silver coating was very weak. Therefore, dense substrates were used for X-ray analysis instead of porous ones. It was reasonable to assume that the coatings on dense and porous substrates had the same microstructure.

X-ray diffraction patterns are shown in Fig. 7. The substrates were coated in the same plating solution for various time up to 6 min. The sharpness of the silver peaks shows that the silver grains are of perfect crystal structure. The intensities of silver peaks increase with the plating time, which is caused by the growth of the silver particles. All the peaks other than those of silver are attributed to Al_2O_3 in the substrates. As can be seen in Fig. 7, the intensities of Al_2O_3 are decreased with the increasing plating time, indicating the growth of silver film. Furthermore, there is no significant peak shift of silver, suggesting a well-crystallized lattice structure.
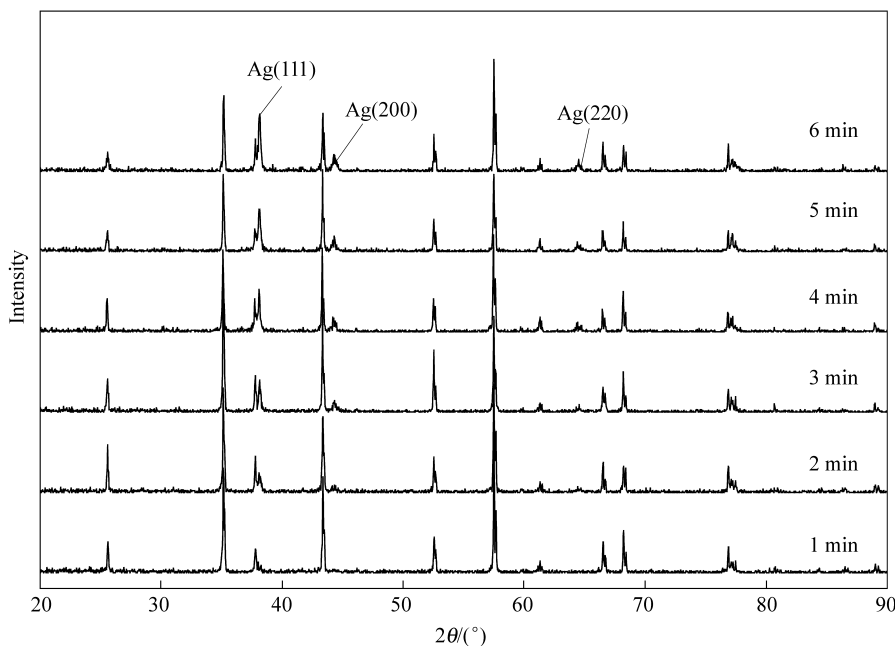

Fig. 7   X-ray diffraction patterns of silver films plated on dense alumina for different time

2.5 Film bond strength

We found that the bond strength between the silver film and the alumina substrate could be well improved by a subsequent sintering process after electroless plating. This was an important step for some practical applications where the frictional force between the flowing liquid and the porous matrix is significant. To examine the bond strength, we employed a standard tape test (ASTM D 3359) which was originally designed for organic coatings on metallic substrate. The tests were performed on dense substrates. Permacel 670 Tape (Permacel, NJ, USA) was used in the test. The tape was pasted on the sintered substrates first and then removed for optical microscopy. The bond strength was

indicated by the amount of particles left on the tape. Fewer particles implied higher strength.

Six dense substrates were plated for 20 min under exactly same condition, and then sintered at different temperatures to test the influence of sintering temperature on the bond strength. All the samples were heated at the rate of 200℃/h to the given temperature, then held for half an hour, and furnace-cooled down to room temperature. Figure 8 shows the tape test results of the relationship between the number of silver particles left on the tapes versus sintering temperature. A great portion of the silver film on the unsintered sample is removed by the testing tape as shown in Fig. 8. However, by sintering the sample at 400℃, number of particles on the tape (NPT) has dropped more than

70%, indicating a significantly increased bonding strength due to sintering. When the sample was sintered to above 600 °C, silver particles were hardly found on the tape. From these results we conclude that sintering could significantly improve the bond strength, especially at higher temperatures.
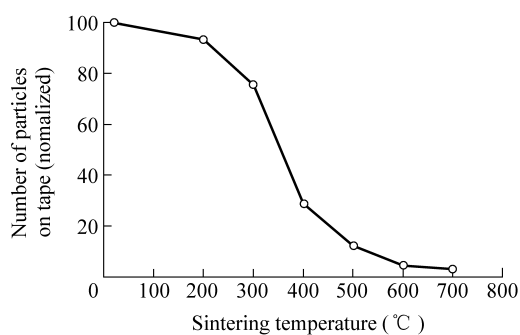

Fig. 8 Number of silver particles left on the tape versus sintering temperature for silver-coated dense alumina

However, the electrical resistivity measurement indicated that the conductivity of the sintered porous substrates decreased sharply at 500 °C at which the bond strength was well-improved (see Fig. 9). But below 400 °C, the resistivity remains almost constant. When the sintering temperature was higher than 600 °C, the sample became insulating.
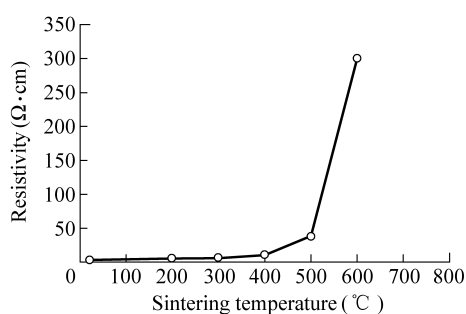

Fig. 9 Resistivity versus sintering temperature for the silver-coated porous alumina

There are two possible factors causing the resistivity to increase during sintering. One is the oxidation of silver; the other is the disruption of the percolation current path due to clustering of silver film. To find out the oxidation state of the silver film, XRD investigation was performed on the sintered samples. Figure 10 shows the XRD results of the sintered dense substrates. As shown in this figure, there are not any characteristic peaks of AgO, and the intensities of Ag(111), Ag(200), and Ag(220) have increased with the sintering

temperature. Based on these results we can rule out the first possibility that silver oxide may have been formed during sintering.
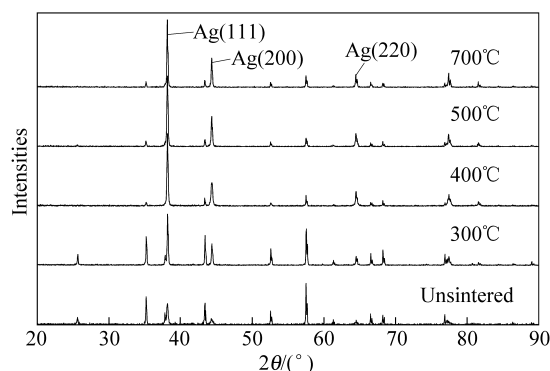

Fig. 10 X-ray diffraction patterns of silver films on dense alumina sintered at different temperatures

Therefore, the only possible reason for the decrease in conductivity may lie on the clustering of silver particle, which could result in the cut-off of the electrical current path. SEM photographs of the sintered samples verified this conjecture. Figures 11a-11d show the coated dense samples sintered at 200 °C, 400 °C, 600 °C, and 700 °C, respectively. For the sample sintered at temperature 200 °C and 400 °C, the samples showed little clustering of silver film, but severe clustering and grain growth were found on the samples sintered at 600 °C and 700 °C. The average grain size increased from 2-3 μm of the unsintered samples to 7-10 μm in the sample sintered at 700 °C, on which the silver grains were separated from each other. This behavior must be responsible for the disruption of the percolation electrical current path, which caused the resistivity to increase rapidly. Though the temperature was much lower than the melting point of metal silver, the grains grew at a considerable rate because of their small sizes. Below 400 °C, silver film clustered slightly, and the conductivity was kept at a high level, while the binding force was improved remarkably. At the higher temperature of 600 °C, the separated island-shaped film segments with smooth edges and surfaces were observed. Although the bonding between the film and the substrate was strong, the film was no longer conductive. Based on these results, the sintering temperature at 400 °C appears to be an optimized one at which the composite is able to exhibit considerable conductivity while maintaining its strong bond between the silver film and the substrate. Therefore, for optimized

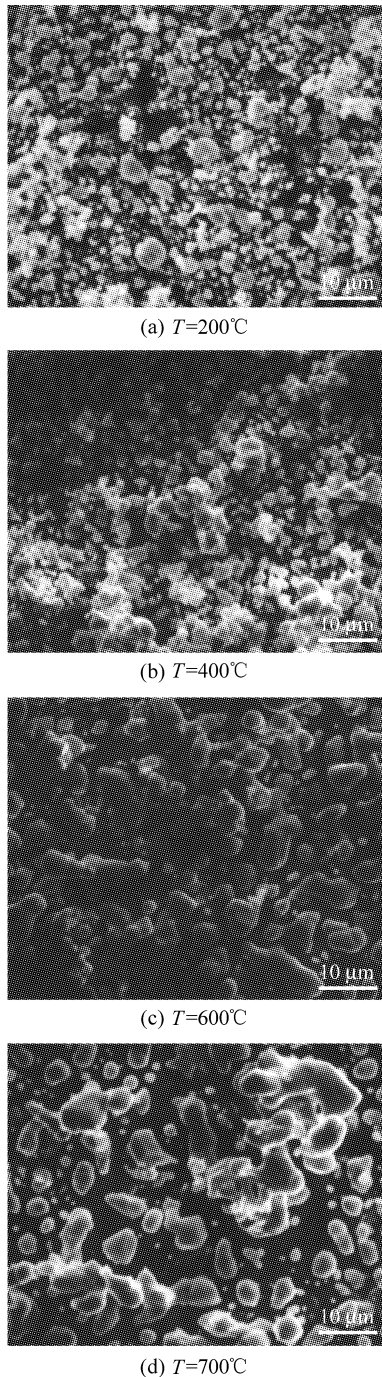properties, the sintering temperature should be near 400°C.

(a) T=200°C

(b) T=400°C

(c) T=600°C

(d) T=700°C

Fig. 11   SEM photographs showing the silver films sintered on dense alumina at different temperatures

2.6   Theoretical modeling of the silver film deposition

As silver deposition is complex and different from any vapor or electro-plating processes, the film formation

modes and thermodynamic conditions deserve special attention and treatment.

All phase transformations, including coating, involve the processes of nucleation and growth. During the earliest stage of film formation, a sufficient number of atoms or molecules condense and establish a permanent residence on the substrate. This is the so-called nucleation stage, followed by the growth stage. However, it is doubtful that there is a clear demarcation between the end of nucleation and the onset of nucleus growth.

Film formation can be classified into three basic categories: 1) island (or Volmer-Weber) mode, 2) layer (or Frank-van der Merwe) mode, 3) Stranski-Krastanov mode, which are shown in Fig. 12[10].
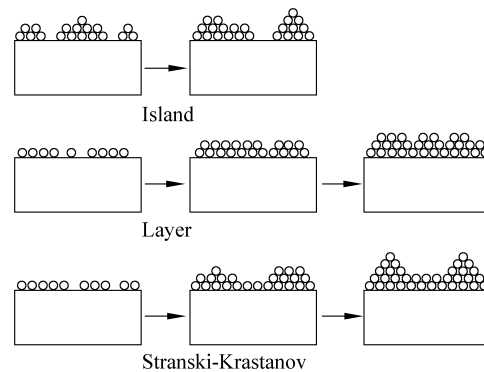

Fig. 12   Schematic diagram of basic modes of thin-film growth

Island growth occurs when the smallest stable clusters nucleate on the substrate and grow in three dimensions to form islands. This happens when atoms or molecules in the deposit are more strongly bound to each other than to the substrate. Many systems of metals on insulators, alkali halide crystals, graphite, and mica substrates display this mode of growth. Silver coating in this study also falls in this category.

In layer growth mode, which is the small stable nucleus growth mainly in two dimensions rather than in three, forming planar sheets. In this mode, the atoms are more strongly bound to substrate than to each other. The first complete monolayer is then covered with a somewhat less tightly bound second layer. The most important examples of this growth mode involve single-crystal epitaxial growth of semiconductors films.

In the Stranski-Krastanov mode, a combination of island and layer mode, after the first layer is formed, subsequent layer growth becomes unfavorable and islands form. The transition from two- to three-

dimensional growth is not completely understood, but any factor that disturbs the monotonic decrease in binding energy characteristic of layer growth may be the cause. This growth mode is fairly common in metal-metal and metal-semiconductor systems.

To further study the theoretical aspect of the growth mode, we have conducted the computational simulation on the model of silver coating. As stated before, the silver coating in this study belongs to the island growth mode. After the substrate is immersed in the plating solution, precipitated silver atoms are distributed randomly onto the substrate surface. Those atoms are highly mobile and can move around within a few micrometers region. If an incoming atom can see another atom or island within its mobility region, it will move to join the cluster to decrease the free energy. In the early stage, the island density is low, coming atoms would rather form new nucleus than join other islands, so the islands grow slowly in size but rapidly in number, but the island density saturates rapidly. In the following stage, most new deposited silver atoms can find a favorable island to join within their mobility. Number of islands is almost fixed, and grows linearly with plating time. The islands keep growing until the main solution depletes. The mobility of the islands decreases with size, so when islands are large to meet each other, they just overlap each other instead of merging.

Based on a physical model, a computer program is developed to simulate the film growth process animatedly. In this program, atoms are randomly deposited onto the substrate surface. Once an atom arrives at the surface, the program will check if there are atoms or islands existing within the mobility of the atom. If it is true, the atom will move toward the nearest atom or island and join it; otherwise, the atom will form a new nucleus by itself. The flowchart of this program is shown in Fig. 13.

The result of the program is shown in Fig. 14. The shot clips taken at increasing coating time matches quite well with the SEM pictures shown in Fig. 4. At first, nuclei are formed rapidly, but little growth occurs (Figs. 14a and 14b). Gradually, nucleation rate decreases while growth rate increases, and in a short time, nuclei saturate and begin to grow fast (Figs. 14c and 14d). Finally the grains are large to touch each other and form a continuous film (Figs. 14e and 14f). A
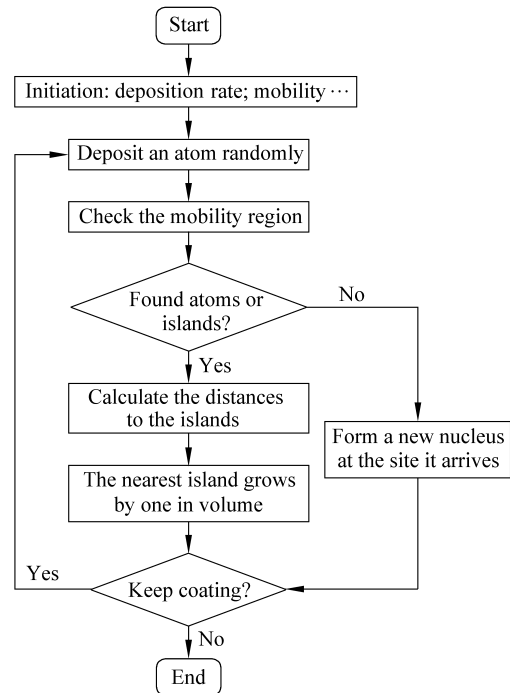

Fig. 13   Flowchart of the simulation program

more complicated program is needed to simulate the final stage after grains meet each other and multiplayer begins to form. Comparison between the simulation and experimental results indicates an excellent description of the coating process by the physical model.

3   Conclusions

We have developed a novel approach to coat inner pore surfaces of the reticulated alumina. We have found that the electroless plating method is suitable for coating a uniform and continuous silver film onto both dense and porous substrates. The optimum silver coating has been achieved by using certain agents and accelerators. The film growth kinetics has been studied by SEM and X-ray diffraction investigations. The relationship between conductivity and silver grain morphology has been established. To improve the silver film bonding to the substrate, sintering at temperatures up to 600°C has been employed which has resulted in greatly improved bonding strength. However, the clustering of the silver particles during sintering has been found to adversely affect the conductivity of the film. An optimized sintering temperature at 400°C has been determined, at which both conductivity and bonding strength are enhanced. The fundamental operating mechanism of silver
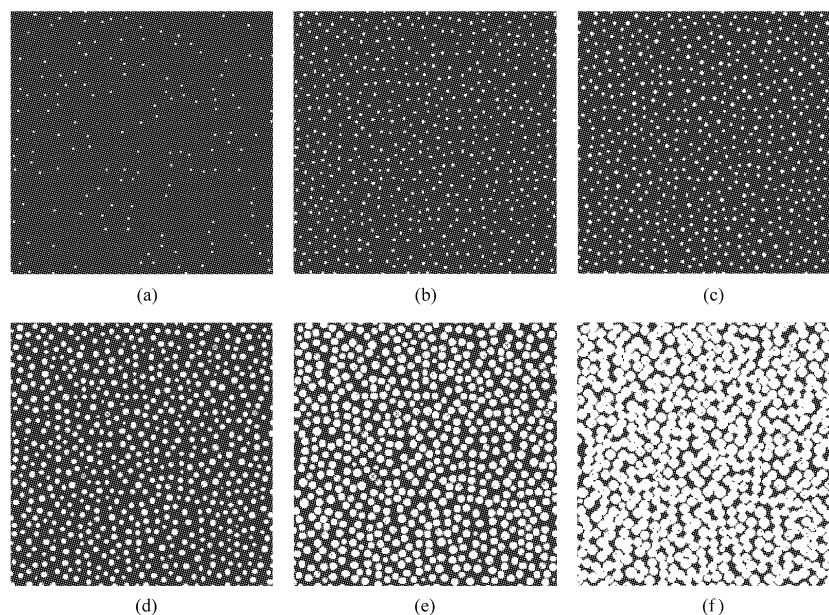
(a)   (b)   (c)

(d)   (e)   (f)

Fig. 14   Simulation of the coating process

electroless plating has been identified. The computer simulation results have shown an excellent agreement between the physical model and the silver deposition behavior.

References

[1]   Jayaraman V, Lin Y S, Pakala M, Lin P Y. Fabrication of ultrathin metallic membranes on ceramic supports by sputter deposition. *J. of Membrane Science*, 1995, **99**: 89-100.

[2]   Padilla A P, Rodriguez J A, Saitua H A. Synthesis and water ulftrafiltration properties of silver membrane supported on porous ceramics. *Desalination*, 1997, **114**: 203-208.

[3]   Jiang Gengwei, Shi Donglu. Coating of hydroxyaptite on highly porous Al$_2$O$_3$ substrate for bone substitute. *J. Biomedical Materials Research (Applied Biomaterials)*, 1998, **43**: 77-81.

[4]   Jiang Gengwei, Shi Donglu. Coating of hydroxyaptite on porous alumina substrate through thermal decompostion. *J. Biomedical Materials Research (Applied Biomaterials)*, 1999, **48**: 117-120.

[5]   Jo Y M, Huchison R, Raper J A. Preparation of ceramic membrane filters, from waste fly ash, suitable for hot gas cleaning. *Waste Management and Research*, 1996, **14**: 281-295.

[6]   Manttari M, Nystrom M, Ekberg B. Influence of flocculants on the filtration of copper concentrates with a ceramic capillary filter. *Minerals Engineering*, 1996, **9**: 419-428.

[7]   Grimm J, Bessarabov D, Sanderson R. Review of electro-assisted methods for water purification. *Desalination*, 1998, **115**: 285-294.

[8]   Saggio-Woyansky J, Scott C E, Minnear W P. Processing of porous ceramics. *American Ceramics Society Bulletin*, 1992, **71**: 1674-1682.

[9]   Vaskelis A, Jagminiene A, Juskenas R, Matulionis E, Norkus E. Structure of electroless silver coatings obtained using cobalt (II) as reducing agent. *Surface and Coatings Technology*, 1996, **82**: 165-168.

[10] Ohring M. The Materials Scinece of Thin Films. London: Academic Press, 1992.